Inorg. Chem. **1992**, *31*, 3295–3301

Design of a Homonuclear Ferromagnetic Chain: Structures and Magnetic Properties of Oxalato-Bridged Copper(II) Complexes with One-Dimensional Structures

Hiroki Oshio*,† **and Umpei Nagashima**

Department of Applied Molecular Science, Institute for Molecular Science, Okazaki 444, Japan

Received November 21, 1991

An orthogonality of magnetic orbitals results in the stabilization of a high spin state, that is, a propagation of a ferromagnetic interaction between magnetic centers. Oxalato-bridged one-dimensional copper(II) complexes $[Cu(en)_2][Cu(ox)_2]$ (**1**) and $[Cu(bpy)(ox)]\cdot 2H_2O$ (**2**) were designed for an each magnetic orbital on adjacent units to be orthogonal, which might result in a ferromagnetic intrachain interaction. In the complex **1**, the oxalato anions are tridentate ligands, and the terminal oxygen atoms of the $[Cu(ox)_2]^{2-}$ unit bridge the adjacent $[Cu(en)_2]^{2+}$ unit from the axial (d_{z^2} orbital) position of the cation. The ground states of the cations and anion units are $d_{x^2-y^2}$. Magnetic susceptibility data have revealed that complex **1** is an antiferromagnetic $S = {}^1/_2$ Heisenberg chain, and exchange coupling constant (J_{AF}) and g values were estimated to be −1.95 (1) cm^{-1} and 2.115 (1), respectively, on the basis of an antiferromagnetic Heisenberg linear chain model. In complex **2**, the oxalato anions are centrosymmetric and act as quadridentate bridging ligands, where the oxygen atoms coordinate to each copper atom both from the equatorial ($d_{x^2-y^2}$ orbital) and axial (d_{z^2} orbital) positions. Magnetic susceptibility data have shown that complex **2** is the ferromagnetic $S = {}^1/_2$ Heisenberg chain, and exchange coupling constant (J_F) and g values were estimated to be 1.22 (4) cm^{-1} and 2.185 (6), respectively, by using a ferromagnetic Heisenberg linear chain model. A magnetization curve of complex **2** at 2 K exhibited more rapid saturation than the calculated curve for $J = {}^3/_2$, where J is the angular momentum quantum number. This ferromagnetic behavior can be readily understood by considering the fact that the spin density on the copper atom is spread over the oxalato groups, as confirmed by the all-electron ab initio unrestricted Hartree–Fock calculation for $[Cu(ox)_2]^{2-}$. The spin on the terminal oxygen atom, which coordinates to the adjacent copper atoms from its d_{z^2} direction, induces spin on that d_{z^2} orbital. The orthogonality of the primary spin orbital ($d_{x^2-y^2}$) and induced spin orbital (d_{z^2}) causes the ferromagnetic interaction. The extended Hückel molecular orbital calculation for $[Cu_2((NH_3)_8(ox)]^{2+}$, which has a coordination geometry similar to that for complex **2**, has shown that the HOMO and LUMO are effectively degenerate (separated by 0.02 eV), and this calculation is in good agreement with the experimental result. Crystal data: $[Cu(en)_2][Cu(ox)_2]$, monoclinic, space group $C2/c$, $a = 14.884$ (2) Å, $b = 12.770$ (2) Å, $c = 7.147$ (1) Å, $\beta = 94.83$ (2)°, $V = 1353.6$ (4) Å^3, $Z = 4$, and $R = 0.026$ ($R_w = 0.035$) for 1938 data with $|F_o| > 3\sigma(F_o)$.

Introduction

In the past decade, a great deal of effort has been devoted to building a molecular-based ferromagnet. Some complexes have been reported to show magnetic ordering below 20 K.[1–4] In order to prepare a complex which exhibits magnetic ordering at higher temperature, three-dimensional magnetic interactions must be made as strong as possible. Molecular engineering techniques for the construction of one-dimensional molecular assemblies might be extended for control of the three-dimensional electronic and magnetic interactions. Several strategies to stabilize the highest spin multiplicity have been proposed: (i) Configuration mixing of a virtual triplet excited state with the ground state between radicals has been suggested.[5,6] Miller and Epstein et al.[1,7,8] have realized this theory in their charge-transfer complex $[Fe(C_5Me_5)_2][TCNE]$ (C_5Me_5 = pentamethylcyclopentadienyl and TCNE = tetracyanoethylene), which exhibits ferromagnetic interaction between radicals. (ii) Strict orthogonality of magnetic orbitals on adjacent paramagnetic centers has also been proposed. The linear chain copper(II) complex bridged by nitronyl nitroxide radical has indicated the stabilization of the highest spin multiplicity due to the orthogonality of magnetic orbitals, i.e., the d_σ and p_π spins on the copper atom and nitronyl nitroxide radical, respectively.[9] The orthogonality of the d_σ and d_π spins has also been used to obtain ferromagnetic interactions in Cr(III)–Ni(II) and Cr(III)–Cu(II) complexes.[10,11] (iii) Strong antiferromagnetic interactions between paramagnetic species with different spin multiplicities, which are alternately aligned, lead to a ferromagnetic like behavior due to the noncompensation of the local spins. O. Kahn et al. have embodied such ferromagnetic like behavior in Mn(II) ($S = {}^5/_2$) and Cu(II) ($S = {}^1/_2$) chain complexes.[2,12–15] Gatteschi et al. have reported that the highest spin multiplicity was stabilized in $M(hfa)_2(NITR)$ (M = Mn and Ni, hfa = hexafluoroacetylacetonato, and NITR = 2-R-4,4,5,5-tetramethyl-4,5-dihydro-1*H*-imidazolyl-1-oxy 3-oxide, where R = methyl, ethyl, propyl, and phenyl) due to the antiferromagnetic coupling between metals and nitronyl nitrox-

---

† Present address: Department of Chemistry, Faculty of Science, Tohoku University, Aoba-ku, Aramaki, Sendai 980, Japan.

(1) Miller, J. S.; Calabrese, J. S.; Rommelmann, H.; Chittipeddi, S. R.; Zhang, J. H.; Reiff, W. M.; Epstein, A. J. *J. Am. Chem. Soc.* **1987**, *109*, 769.

(2) Kahn, O.; Pei, Y.; Verdaguer, M.; Renard, J. P.; Sletten, J. *J. Am. Chem. Soc.* **1988**, *110*, 782.

(3) Canseschi, A.; Gatteschi, D.; Renard, J. P.; Rey, P.; Sessoli, R. *Inorg. Chem.* **1989**, *28*, 1976.

(4) Canseschi, A.; Gatteschi, D.; Renard, J. P.; Rey, P.; Sessoli, R. *Inorg. Chem.* **1989**, *28*, 2940.

(5) McConnell, H. M. *Proc. R. A. Welch Found. Chem. Res.* **1967**, *11*, 144.

(6) Breslow, R. *Pure Appl. Chem.* **1982**, *54*, 927.

(7) Miller, J. S.; Epstein, A.; Reiff, W. M. *Acc. Chem. Res.* **1988**, *21*, 114.

(8) Miller, J. S.; Epstein, A.; Reiff, W. M. *Science* **1988**, *240*, 40.

(9) Caneschi, A.; Gatteschi, D.; Laugier, J.; Rey, P. *J. Am. Chem. Soc.* **1987**, *109*, 2191.

(10) Pei, Y.; Journaux, Y.; Kahn, O. *Inorg. Chem.* **1989**, *28*, 100.

(11) Zhong, Z. J.; Matsumoto, N.; Okawa, H.; Kida, S. *Chem. Lett.* **1990**, 87.

(12) Nakatani, K.; Carriat, J. Y.; Kahn, O.; Lloret, F.; Renard, J. P.; Pei, Y.; Sletten, J.; Verdaguer, M. *J. Am. Chem. Soc.* **1989**, *111*, 5739.

(13) Lloret, F.; Nakatani, K.; Journaux, Y.; Kahn, O.; Pei, Y.; Renard, J. P. *J. Chem. Soc., Chem. Commun.* **1988**, 642.

(14) Pei, Y.; Verdaguer, M.; Kahn, O.; Sletten, J.; Renard, J. P. *Inorg. Chem.* **1987**, *26*, 138.

(15) Pei, Y.; Kahn, O.; Sletten, J.; Renard, J. P.; Georges, R.; Gianduzzo, J. C.; Curley, J.; Xu, Q. *Inorg. Chem.* **1988**, *27*, 47.

0020-1669/92/1331-3295$03.00/0

ide radical centers.[3,4,16,17] All examples described above consist of heteronuclear or heteroparamagnetic species. Some homometal one-dimensional systems with a ferromagnetic intrachain interaction have been reported.[18-23] However, the strategy to build a homonuclear one-dimensional system with stronger ferromagnetic interaction has not been established yet. In this paper, we describe a design of a homometal (copper(II)) ferromagnetic chain system.

Experimental Section

Compound Preparation. Synthesis of [Cu(en)$_2$][Cu(ox)$_2$] (1). All chemicals were of reagent grade and were used as commercially obtained. To a solution of K$_2$[Cu(ox)$_2$]·2H$_2$O[24] (0.2 mmol) in boiling methanol (100 mL) was added a solution of [Cu(en)$_2$](NO$_3$)$_2$·2H$_2$O[25] (0.2 mmol) in methanol (10 mL). Blue precipitates were filtered off and washed with methanol. Crystals for the X-ray crystallographic analysis were grown by the slow diffusion method using a [Cu(en)$_2$](NO$_3$)$_2$ and K$_2$[Cu(ox)$_2$] methanol solution. Anal. Calcd for $C_8H_{16}N_4O_8Cu_2$ (**1**): C, 22.70; H, 3.81; N, 13.23. Found: C, 22.81; H, 3.79; N, 13.25.

Synthesis of [Cu(bpy)(ox)]·2H$_2$O (2). The compound were prepared by the procedure given by Hathaway et al.[26] Slow evaporation of the methanol solution resulted in blue crystals for X-ray analysis. Anal. Calcd for $C_{12}H_{12}N_2O_6Cu$ (**2**): C, 41.93; H, 3.52; N, 8.15. Found: C, 41.75; H, 3.70; N, 8.24.

Magnetic Measurements. Variable-temperature dependences of magnetic susceptibilities of powdered samples were measured by an Oxford Faraday type magnetic balance system equipped with a superconducting magnet. Temperature readings were calibrated with a magnetic thermometer by the use of Cr(NH$_3$)$_6$Cl$_3$. All data were corrected for diamagnetism.[27] Least-squares fitting of the magnetic susceptibility to approximate equations for the ferro- or antiferromagnetic chain were performed with the least-squares program Igor on a Macintosh computer.

Molecular Orbital Calculations. All-electron ab initio unrestricted Hartree–Fock (UHF) calculations for [Cu(ox)$_2$]$^{2-}$ were carried out by using the GAUSSIAN82 program.[28] The basis set for the ^{2}D state of the copper atom given by Roos et al.[29] is constructed as [5s, 2p, 1d], and p and d type polarization functions ($\zeta = 0.25$ and 0.1682, respectively)[30,31] are added to the basis set. STO-3G[32] minimal basis sets were adopted for the carbon and oxygen atoms. The structural parameters obtained by X-ray analysis were employed with a few adjustments to obtain the D_{2h} symmetry. Extended Hückel molecular orbital (EHMO) calculations[33,34] were done for the dinuclear copper(II) complex. The parameters for the EHMO calculation were taken from references,[35,36] and geometries used will be mentioned in the text.

Table I. Crystallographic Data for [Cu(en)$_2$][Cu(ox)$_2$] (**1**)

formula	$C_8H_{16}Cu_2N_4O_8$
fw	423.3284
temp (°C)	20
cryst system	monoclinic
space group	*C*2/*c*
a (Å)	14.884 (2)
b (Å)	12.770 (2)
c (Å)	7.147 (1)
β (deg)	94.83 (2)
V (Å^3)	1353.6 (4)
Z	4
D_c (g cm^{-3})	2.077
μ(Mo Kα) (cm^{-1})	33.1414
R^a	0.026
$R_w{}^b$	0.035

[a] $R = \sum(|F_o| - |F_c|)/\sum|F_o|$. [b] $R_w = [\sum w(|F_o| - |F_c|)^2/\sum w|F_o|^2]^{1/2}$; $w = 1/\sigma^2(|F_o|)$.

Table II. Positional (×10^4) and Equivalent Isotropic Thermal Parameters (Å^2) for [Cu(en)$_2$][Cu(ox)$_2$] (**1**)

	x	*y*	*z*	$B_{eq}{}^a$
Cu(1)	2500	2500	5000	1.9
Cu(2)	0	0	0	1.9
O(1)	981 (1)	62 (1)	−1650 (2)	2.2
O(2)	181 (1)	1495 (1)	207 (2)	2.4
O(3)	1963 (1)	1207 (1)	−2638 (2)	3.0
O(4)	1170 (1)	2723 (1)	−474 (2)	2.8
N(1)	1268 (1)	2916 (1)	3832 (2)	2.2
N(2)	2340 (1)	3692 (1)	6768 (2)	2.2
C(1)	900 (1)	3760 (2)	4945 (3)	2.8
C(2)	1670 (1)	4408 (2)	5851 (3)	2.6
C(3)	1333 (1)	980 (1)	−1736 (2)	1.8
C(4)	871 (1)	1827 (1)	−577 (2)	1.8

[a] The equivalent isotropic temperature factor is calculated using the expression $B_{eq} = (4/3)\sum_i\sum_j a_i a_j \beta_{ij}$, where a_i's are the unit cell edges in direct space.

Data Collection and Processing. Blue crystals (0.38 × 0.14 × 0.07 mm^3 for complex **1** and 0.40 × 0.18 × 0.22 mm^3 for complex **2**) were attached to the end of glass fibers and mounted on a Rigaku AFC-5R four-circle diffractometer. Crystallographic data and data collection parameters are summarized in Tables I and SVII (supplementary material). Intensity data were obtained by use of an ω–2θ scan using graphite-monochromated Mo Kα radiation: 2712 and 5419 reflections ($2° < 2\theta < 65°$, $-22 < h < 22$, $0 < k < 19$, $0 < l < 11$; $2° < 2\theta < 60°$, $-14 < h < 14$, $-14 < k < 14$, $0 < l < 13$) were measured for **1** and **2**, respectively, of which 1938 and 4161 were respectively observed [$|F_o| > 3\sigma(F_o)$]. The intensities were corrected for Lorentz–polarization and absorption effects but not for extinction. Lattice constants were determined by a least-squares refinement based on 50 reflections ($12° < \theta < 15°$) measured on the diffractometer.

Structure Analysis and Refinement. The structures were solved by the conventional heavy-atom method and refined by a block-diagonal least-squares technique with anisotropic thermal parameters for non-H atoms and isotropic for H atoms. Atomic scattering factors and anomalous scattering corrections were taken from the literature.[37] The weighting schemes chosen for the compounds **1** and **2** were $w = [\sigma_c{}^2 + (0.015|F_o|)^2]^{-1}$ and $w = [\sigma_c{}^2 + (0.030|F_o|)^2]^{-1}$, respectively, where $\sigma_c{}^2$ was the standard deviation of $|F_o|$ calculated from counting statistics. The final atomic parameters and equivalent isotropic thermal factors for non-hydrogen atoms are listed in Tables II and SVIII (supplementary material).

All calculations were carried out on a HITAC M680 computer at the Computer Center of the Institute for Molecular Science with the Universal Crystallographic Computation Program System UNICS-III.[38]

---

(16) Canseschi, A.; Gatteschi, D.; Renard, J. P.; Rey, P. *J. Am. Chem. Soc.* **1989**, *111*, 785.

(17) Caneschi, A.; Gatteschi, D.; Rey, P.; Sessoli, R. *Inorg. Chem.* **1988**, *27*, 1756.

(18) Willett, R. D.; Gaura, R. M.; Landee, C. P. In *Extended Linear Chain Compounds*; Miller, J. S., Ed.; Plenum: New York, London, 1983; Vol. 3, p 143.

(19) Hatfield, W. E.; Estes, W. E.; Marsch, W. E.; Pickens, M. W.; Ten Haar, L.; Weller, R. R. In *Extended Linear Chain Compounds*; Miller, J. S., Ed.; Plenum: New York, London, 1983; Vol. 3, p 43.

(20) Towle, D. K.; Hoffmann, S. K.; Hatfield, W. E.; Singh, P.; Chaudhuri, P. *Inorg. Chem.* **1988**, *27*, 394.

(21) Corvan, P.; Estes, W. E.; Weller, R. R.; Hatfield, W. E. *Inorg. Chem.* **1980**, *19*, 1297.

(22) O'Connor, C. J.; Klein, C. L.; Majeste, R. J.; Trefonas, L. M. *Inorg. Chem.* **1982**, *21*, 64.

(23) Geiser, U.; Ramakrishna, B. L.; Willett, R. D.; Hulsbergen, F. B.; Reedijk, J. *Inorg. Chem.* **1987**, *26*, 3750.

(24) Kirschner, S. *Inorganic Syntheses*; Rochow, E. G., Ed.; McGraw-Hill Book Co.: New York, 1960; Vol. VI, p 1.

(25) Portillo, R. *Chem. Abstr.* **1930**, *24*, 308.

(26) Fitzgerald, W.; Foley, J.; McSweeney, D.; Ray, N.; Sheahan, D.; Tyagi, S.; Hathaway, B. *J. Chem. Soc., Dalton Trans.* **1982**, 1117.

(27) Earnshaw, A. *Introduction to Magnetochemistry*; Academic Press: London, 1968.

(28) Binkley, J. S.; Frish, M.; Reghavachari, K.; DeFrees, D.; Schlegel, H. B.; Whiteside, R.; Fluder, E.; Seeger, R.; Pople, J. A. Carnegie-Mellon Quantum Chemistry Archive, Carnegie-Mellon University, Pittsburgh, PA, 1983.

(29) Roos, B.; Veillard, A.; Virot, G. *Theor. Chim. Acta* **1971**, *20*, 1.

(30) Hay, P. J. *J. Chem. Phys.* **1977**, *66*, 4377.

(31) Jensen, J. R.; Fenske, R. F. *Theor. Chim. Acta* **1978**, *48*, 241.

(32) Hehre, W. J.; Stewart, R. F.; Pople, J. A. *J. Chem. Phys.* **1969**, *51*, 2657.

(33) Hoffmann, R. *J. Chem. Phys.* **1963**, *39*, 1397.

(34) Hoffmann, R.; Lipscomb, W. N. *J. Chem. Phys.* **1962**, *36*, 2179.

(35) Hay, P. J.; Thibeault, J. C.; Hoffmann, R. *J. Am. Chem. Soc.* **1975**, *97*, 4884.

(36) Summerville, R. H.; Hoffmann, R. *J. Am. Chem. Soc.* **1976**, *99*, 7240.

(37) *International Tables for X-ray Crystallography*; Kynoch Press: Birmingham, England, 1982; Vol. IV.

(38) Sakurai, T.; Kobayashi, K. *Sci. Rep. Inst. Chem. Phys. Res.* (*Jpn.*) **1979**, *55*, 69.

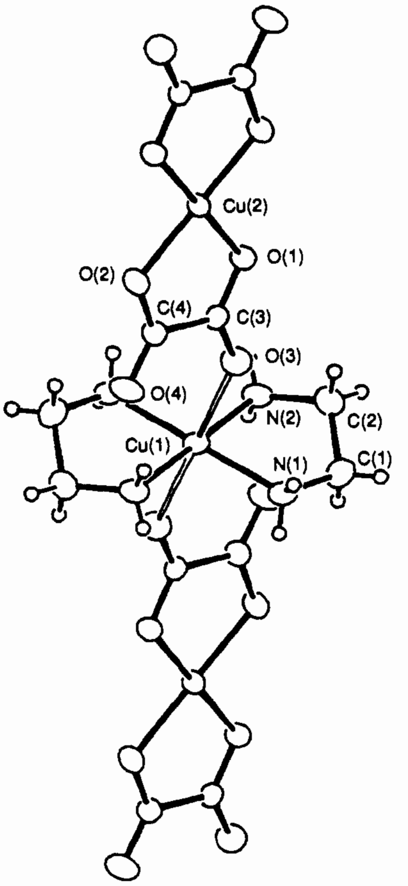

Figure 1. View of the $[Cu(en)_2][Cu(ox)_2]$ chain with 50% probability.

Table III. Selected Bond Lengths (Å) and Angles (deg) of $[Cu(en)_2][Cu(ox)_2]$ (**1**)[a]

Cu(1)–N(1)	2.021 (2)	Cu(1)–N(2)	2.005 (2)
Cu(1)–O(3)^a	2.539 (2)	Cu(2)–O(1)	1.954 (2)
Cu(2)–O(2)	1.932 (1)	Cu(1)–Cu(2)	5.8795 (9)
O(3)^a–Cu(1)–N(1)	96.91 (6)	O(3)^a–Cu(1)–N(1)^b	83.09 (6)
O(3)^a–Cu(1)–N(2)	90.80 (6)	O(3)^a–Cu(1)–N(2)^b	89.20 (6)
O(3)^b–Cu(1)–O(3)	180.0	N(1)–Cu(1)–N(2)	84.80 (7)
N(1)–Cu(1)–N(2)^b	95.20 (7)	O(1)–Cu(2)–O(2)	84.25 (6)
O(1)–Cu(2)–O(2)^c	95.75 (6)		

[a] Key to symmetry operations: (a) $x, y, 1 - z$; (b) $^1/_2 - x, ^1/_2 - y, 1 - z$; (c) $-x, -y, -z$.

Results

Structure of $[Cu(en)_2][Cu(ox)_2]$ (1). The blue crystal consists of $[Cu(en)_2]^{2+}$ and $[Cu(ox)_2]^{2-}$ ions. The crystal structure is a polymeric structure and comprised of bridged $[Cu(en)_2]^{2+}$ and $[Cu(ox)_2]^{2-}$ units. An ORTEP drawing of the one-dimensional structure is depicted in Figure 1. Selected bond lengths and angles are listed in Table III. The copper atoms both in the cation and anion are located at a center of symmetry. The coordination geometry of the cation $[Cu(en)_2]^{2+}$ is that of a six-coordinate CuN_4O_2. The equatorial plane consists of four nitrogen atoms of ethylenediamine, and the two axial positions are occupied by terminal oxygen atoms of the adjacent anions. The bond lengths between the copper and the equatorial nitrogen atoms (2.021 and 2.005 Å) are shorter than those between copper and the axial oxygen atoms (2.539 Å) as expected for a six-coordinate copper(II) complex. The coordination geometry of the complex anion $[Cu(ox)_2]^{2-}$ is expressed as a four-coordinated square plane. Four oxygen atoms of the two oxalato groups coordinate to the copper ion. The terminal oxygen atoms of each oxalate, which are related by a crystallographic center of symmetry, coordinate to the copper atom of the adjacent $[Cu(en)_2]^{2+}$ unit forming a chain structure. The ground states (magnetic orbitals) of both of the copper atoms are described as $d_{x^2-y^2}$. The copper ion in the cation is separated from the copper atom in the anion by a distance of 5.8795 (9) Å.

Table IV. Selected Bond Lengths (Å) and Angles (deg) of $[Cu(bpy)(ox)]\cdot 2H_2O$ (**2**)[a]

Cu–O(1)	1.984 (2)	Cu–O(2)	1.993 (1)
Cu–N(1)	2.012 (1)	Cu–N(2)	1.998 (2)
Cu–O(3)^a	2.313 (2)	Cu–O(4)^b	2.314 (2)
Cu–Cu^b	5.5567 (8)		
O(1)–Cu–O(2)	90.31 (5)	O(1)–Cu–N(1)	94.02 (6)
O(1)–Cu–N(2)	173.67 (6)	O(1)–Cu–O(3)^a	77.89 (6)
O(1)–Cu–O(4)	89.95 (6)	O(2)–Cu–N(1)	175.64 (7)
O(2)–Cu–N(2)	94.93 (6)	O(2)–Cu–O(3)^a	85.74 (5)
O(2)–Cu–O(4)	77.50 (5)	N(1)–Cu–N(2)	80.72 (6)
N(1)–Cu–O(3)^a	94.67 (6)	N(1)–Cu–O(4)	102.97 (6)
N(2)–Cu–O(3)^a	98.92 (7)	N(2)–Cu–O(4)	94.66 (6)
O(3)*–Cu–O(4)	159.26 (5)		

[a] Key to symmetry operation: (a) $-x, -y, 1 - z$; (b) $-x, -y, -z$.

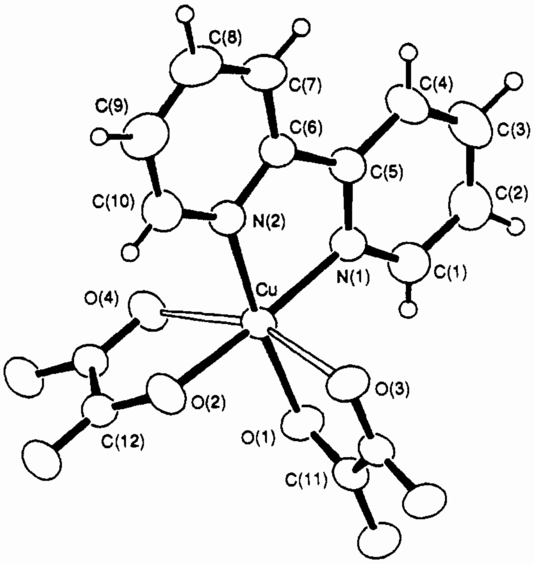

Figure 2. ORTEP diagram of [Cu(bpy)(ox)] with 50% probability.

Structure of $[Cu(bpy)(ox)]\cdot 2H_2O$ (2). The crystal structure of complex **2** was identical with the compound prepared by Hathaway et al.[26] ORTEP drawings of the molecule with the atomic labeling system and the projection view on the *bc*-plane are presented in Figures 2 and 3, respectively. Selected bond lengths and angles are listed in Table III. The crystal structure is composed of polymeric chains of $[Cu(bpy)]^{2+}$ ions bridged by oxalato anions. The copper atom is coordinated by two nitrogen atoms of the bipyridine and four oxygen atoms of the two oxalato groups, and the coordination geometry of the copper atom is described by an elongated rhombic octahedron. The oxalato groups are centrosymmetric and involved in an asymmetric bridge between center-related copper atoms, which form a zigzag chain structure. According to the bond lengths between the copper and coordinating atoms (i.e., four bonds with short bond distances (1.984–2.012 Å) and two bonds with long bond distances (2.313 and 2.314 Å)), a basal plane for the octahedron is regarded as the plane defined by the O(1), O(2), N(1), and N(2) atoms. The coordination angles about the copper atom in the basal plane are close to 90°, and this result implies that the ground state of the copper atom can be expressed as $d_{x^2-y^2}$ with a slight mixing of the d_{z^2} state. Two copper atoms are separated by 5.5567 (8) Å.

Magnetic Properties. Cryogenic magnetic susceptibilities of both complexes **1** and **2** were measured down to 1.9 K, and the $\chi_m T$ vs temperature plots, where χ_m is the molar magnetic susceptibility, are depicted in Figure 4. Small humps appearing in the temperature range from 30 to 50 K in both the complexes are due to absorbed oxygen. The temperature dependence of the product of susceptibility χ_m and temperature T values can be

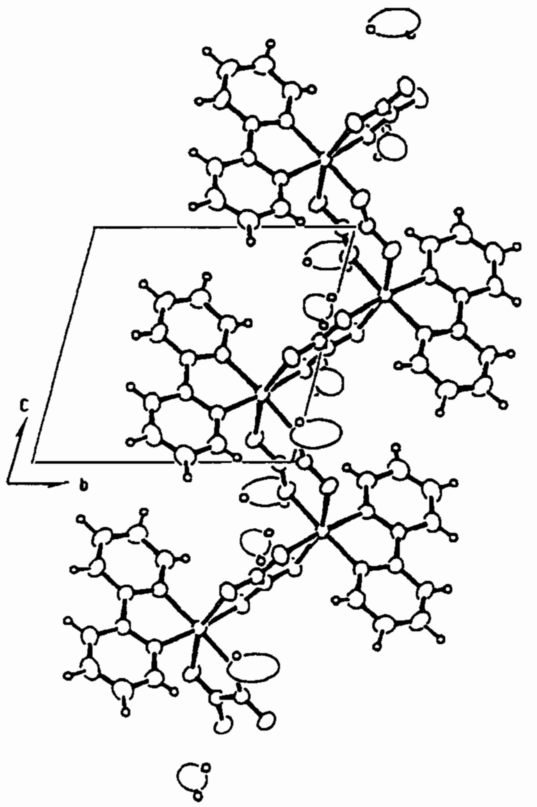

Figure 3. Projection view of [Cu(bpy)(ox)]·$2H_2O$.

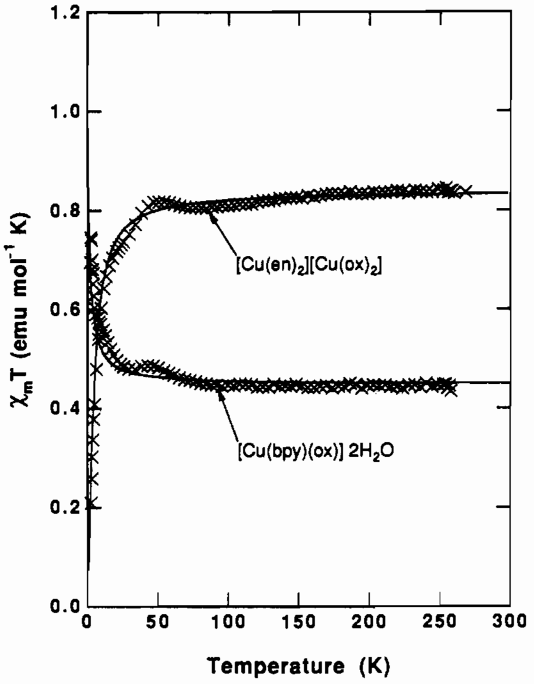

Figure 4. Experimental (×) and calculated (—) temperature dependences of χ_mT for [Cu(en)$_2$][Cu(ox)$_2$] and [Cu(bpy)(ox)]·$2H_2O$.

informative about the magnetic interaction between paramagnetic centers. If the χ_mT values decrease with a decrease in temperature, this indicates an antiferromagnetic interaction. On the other hand, if the χ_mT values increase with a decrease in temperature, the magnetic interaction is ferromagnetic.

The χ_mT values for complex **1** show a gradual decrease upon cooling, and this behavior can be interpreted by the existence of an antiferromagnetic interaction between copper centers. X-ray crystallographic analysis has shown that the copper atoms in complex **1** are alternately arranged, so the magnetic susceptibility data were analyzed by the intrachain exchange model, which has been studied by Duffy and Bar.[39] The isotropic Hamiltonian is expressed as

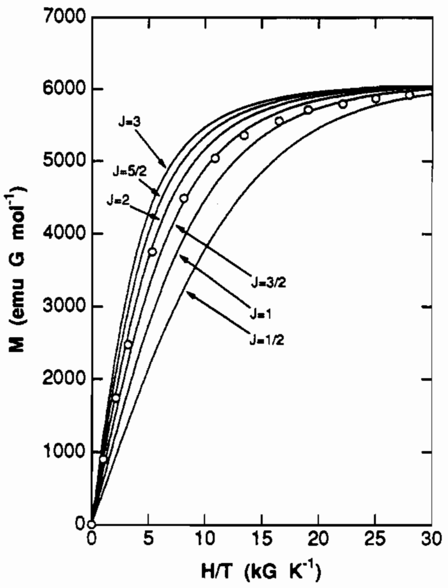

Figure 5. Plots of magnetization (M) vs field strength (H/T) for [Cu(bpy)(ox)]·$2H_2O$ at 2 K. Solid lines are given by the Brillouin function with $J = {}^1/_2, 1, {}^3/_2, 2, {}^5/_2$, and 3.

$$H = -2J\sum_{i=1}^{n/2}[S_{2i}S_{2i-1} + \alpha S_{2i}S_{2i+1}]$$

where J is the exchange integral coupling of a spin with its nearest neighbor and αJ is the exchange integral of a spin with its other neighbor, and $|\alpha| < 1$. Hatfield et al. have reported the recalculation for the model by Duffy and Barr and have obtained numerical data for the generation of the magnetic susceptibility in terms of the exchange coupling constant J and the alternation parameter α.[40-42] The reduced susceptibility is expressed as

$$\chi_m = \frac{Ng^2\mu_B{}^2}{k_BT}\,\frac{A + Bx + Cx^2}{1 + Dx + Ex^2 + Fx^3} \qquad (1)$$

where g is the g factor, μ_B is the Bohr magnetron, k_B is the Boltzmann constant, $x = -J_{AF}/k_BT$, and constants A–F are power series in terms of α. The best fit of eq 1 to the data of complex **1** was obtained with $J_{AF} = -1.95$ (1) cm^{-1} and $g = 2.115$ (2), where α is fixed to 1 because of the alternate arrangement of the copper atoms.

The product of χ_m and temperature values for complex **2** shows a gradual increase as the temperature is decreased. This magnetic behavior does indicate the existence of the ferromagnetic interaction between metal centers. The result of magnetization experiments as a function of applied field at 2 K is shown in Figure 5 along with theoretical curves given by Brillouin function ($B_J(x)$). The magnetization is expressed as

$$M = M_sB_J(x) \qquad x = Jg\mu_BH/k_BT$$

where M_s is the saturation magnetization and J is the quantum number of the total angular momentum. In this calculation, the g value was fixed to 2.176, which was estimated from the Curie constant. The experimental magnetization values at 2 K are greater than the predicted values by the Brillouin function for the $J = {}^3/_2$ system, and this supports the existence of the ferromagnetic interaction.

---

(39) Duffy, W.; Barr, K. P. *Phys. Rev.* **1968**, *165*, 647.

(40) Hall, J. W.; Marsh, W. E.; Weller, R. R.; Hatfield, W. E. *Inorg. Chem.* **1981**, *20*, 1033.

(41) Chiari, B.; Hatfield, W. E.; Piovesana, O.; Tarantelli, T.; Haar, L. W.; Zanazzi, P. F. *Inorg. Chem.* **1983**, *22*, 1468.

(42) Hatfield, W. E. *J. Appl. Phys.* **1981**, *52*, 1985.

The magnetic susceptibility data of complex **2** were analyzed by the Heisenberg linear chain model. The Hamiltonian is

$$H = -2J\sum_{i} S_i S_{i+1}$$

where J is the intrachain-exchange coupling constant and the summation is over all members of the chain. The equation based on the high-temperature Padé expansion by Baker et al.[43] was used to fit the data. The equation for a $S = {}^1/_2$ chain is

$$\chi_m = Ng^2\mu_B^{\,2}\left[\frac{1 + a_1K + a_2K^2 + a_3K^3 + a_4K^4 + a_5K^5}{1 + b_1K + b_2K^2 + b_3K^3 + b_4K^4}\right]^{2/3} \quad (2)$$

where $K = J_F/2k_BT$ and a_i and b_i are expansion coefficients. In this calculation, the interchain magnetic interaction was ignored. Experimental data above 11 K of complex **2** were fitted to eq 2 by a least-squares method. The J_F and g values for complex **2** were evaluated to be +1.22 (4) cm^{-1} and 2.185 (6), respectively.

Discussion

In order to construct a molecular-based ferromagnet, it is necessary to control the two- or three-dimensional magnetic interactions. Some of the compounds referred to in the Introduction have been shown to exhibit magnetic ordering.[1-4] All such systems consist of heteronuclear systems, if organic radicals are considered as having a heteronucleus. Is it possible to build a homometal ferromagnet or even to prepare a homometal one-dimensional ferromagnetic chain?

In a dinuclear system, the interaction of the magnetic orbitals ($d^A_{x^2-y^2}$ and $d^B_{x^2-y^2}$) on each copper atom forms bonding and antibonding molecular orbitals ($\phi_1 = d^A_{x^2-y^2} + d^B_{x^2-y^2}$ and $\phi_2 = d^A_{x^2-y^2} - d^B_{x^2-y^2}$), which correspond to the HOMO and LUMO, respectively. The triplet–singlet state energy difference ΔE ($=E_T - E_S$) is expressed as[36]

$$E_T - E_S = -2K_{ab} + \frac{2(\epsilon_1 - \epsilon_2)^2}{J_{aa} - J_{ab}} \quad (3)$$

where K_{ab}, J_{aa}, and J_{ab} are the exchange integral and one-center and two-center Coulomb repulsion integrals, respectively, and ϵ_1 and ϵ_2 are the energy levels of the HOMO and LUMO. The value of K_{ab} is always positive, so the first term in eq 3 contributes to the ferromagnetic interaction, while the second term, which is always positive, contributes to the antiferromagnetic interaction. The energy difference between two molecular orbitals $\Delta\epsilon$ ($=\epsilon_1 - \epsilon_2$), which corresponds to the HOMO–LUMO energy gap, determines the magnitude of the antiferromagnetic interaction. The stronger antiferromagnetic interaction is expected for the system with the larger HOMO–LUMO energy gap. The numerator of the second term ($(\epsilon_1 - \epsilon_2)^2$) is proportional to the overlap integral between the magnetic orbitals (ϕ_1 and ϕ_2). The triplet state is stabilized if the numerator becomes zero, that is, the magnetic orbitals are orthogonal. It can be also expected that the ferromagnetic interaction is favored if the second term is small enough compared with the first term. The above question is equivalent to asking whether the magnetic orbitals on adjacent metal centers can be orthogonally aligned or the HOMO–LUMO energy gap can be made small enough.

First we have to select a proper metal ion and an appropriate bridging ligand in order to realize a strong magnetic interaction in the chain system. Perturbation theory predicts that two orbitals can strongly interact if the orbitals have the same symmetries and comparable energies. That is, magnetic d-orbitals and p-orbitals of the bridging ligand should have the same symmetry and should be close in energy in order to possess a strong magnetic interaction through the bridging ligand. Ab initio molecular orbital calculations of the divalent metal oxides have proven that the energy level of the d-orbitals of the copper ion is the closest to the oxygen p-orbital among the first row transition metal ions.[44] In addition, the oxalato ligand is known to propagate a strong magnetic interaction in some dinuclear copper(II) complexes.[45,46] Thus, we selected the Cu(ox) unit as a component of the one-dimensional compound.

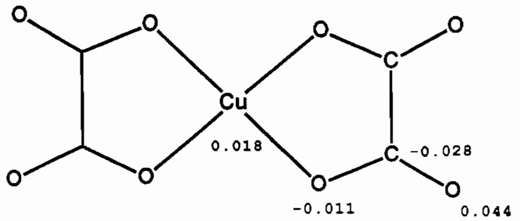

Figure 6. Fermi contact terms of $[Cu(ox)_2]^{2-}$ obtained by the all-electron ab initio unrestricted Hartree–Fock calculation.

Table V. Orbital Populations and Fermi Contact Analysis Obtained by the All-Electron ab Initio Unrestricted Hartree–Fock Calculation for $[Cu(ox)_2]^{2-}$

atom	orbital	gross orbital populations	Fermi contact term (au)
Cu	3s	0.0	0.018
	4s	−0.02	
	$2p_x$	0.0	
	$2p_y$	0.0	
	$2p_z$	0.0	
	$3p_x$	−0.01	
	$3p_y$	−0.01	
	$3p_z$	−0.01	
	$1d_0$	0.0	
	$1d_{+1}$	0.0	
	$1d_{-1}$	0.91	
	$1d_{+2}$	0.01	
	$1d_{-2}$	0.0	
	$2d_0$	0.0	
	$2d_{+1}$	0.0	
	$2d_{-1}$	−0.02	
	$2d_{+2}$	0.0	
	$2d_{-2}$	0.0	
O(1)	2s	0.0	−0.011
	$1p_x$	−0.13	
	$1p_y$	0.02	
	$1p_z$	0.02	
C(1)	2s	−0.02	−0.028
	$1p_x$	−0.16	
	$1p_y$	0.0	
	$1p_z$	−0.01	
O(2)	2s	0.01	0.044
	$1p_x$	0.29	
	$1p_y$	0.0	
	$1p_z$	0.02	

In complex **1**, the ground states both of the $[Cu(en)_2]^{2+}$ and $[Cu(ox)_2]^{2-}$ ions are $d_{x^2-y^2}$. $[Cu(en)_2]^{2+}$ is a square planar complex and has two additional (axial) coordination sites; i.e., a d_{z^2} direction. An X-ray crystallographic study has revealed that complex **1** has a chain structure where the terminal oxygen atoms of $[Cu(ox)_2]^{2-}$ coordinate to the $[Cu(en)_2]^{2+}$ ion from the axial positions of the cation. An all-electron ab initio unrestricted Hartree–Fock (UHF) calculation for $[Cu(ox)_2]^{2-}$ revealed a substantial spin delocalization throughout the whole molecule (Table V and Figure 6), so the terminal oxygen atom of the $[Cu(ox)_2]^{2-}$ unit has a substantial spin density. It can be expected

---

(43) Baker, G. A.; Rushbrooke, G. S.; Gilbert, H. E. *Phys. Rev.* **1964**, *135*, A1272.

(44) Yamaguchi, K.; Nakano, M.; Namimoto, H.; Fueno, T. *Jpn. J. Appl. Phys.* **1988**, *27*, L1835.

(45) Kahn, O. *Angew. Chem., Int. Ed. Engl.* **1985**, *24*, 834.

(46) Benchini, A.; Bianchi, A.; Garacria-Espana, E.; Jeannin, Y.; Julve, M.; Marcelino, V.; Philoche-Levisalles, M. *Inorg. Chem.* **1990**, *29*, 963.

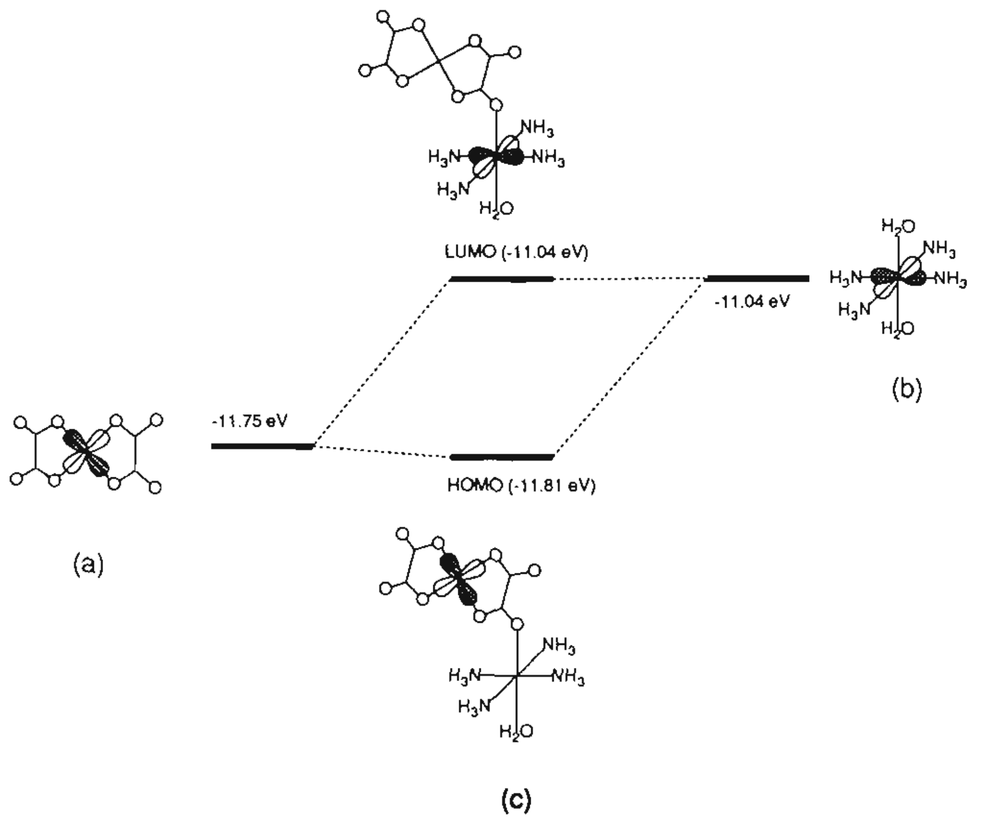

Figure 7. Extended Hückel MO diagrams of (a) $[Cu(ox)_2]^{2-}$, (b) $[Cu(NH_3)_4(H_2O)_2]^{2+}$, and (c) $[Cu(NH_3)_4(H_2O)][Cu(ox)_2]$.

that the spin on the terminal oxygen atoms might induce a spin on the d_{z^2} orbital of $[Cu(en)_2]^{2+}$.[47] If so, it is expected that the orthogonality of the induced spin (d_{z^2}) and the spin of the $d_{x^2-y^2}$ orbital in the $[Cu(en)_2]^{2+}$ unit should result in a ferromagnetic interaction. Magnetic susceptibility data have shown that the magnetic interaction of $[Cu(en)_2][Cu(ox)_2]$ is unexpectedly antiferromagnetic ($J_{AF} = -1.95$ (1) cm^{-1}). The weak antiferromagnetic interaction of complex **1** can be explained by the long Cu(1)–O(3) bond length (2.539 (3) Å), which causes a small induction of the spin on the d_{z^2} orbital of $[Cu(en)_2]^{2+}$. We have done extended Hückel molecular orbital (EHMO) calculations on a dimer unit $[Cu(NH_3)_4(H_2O)][Cu(ox)_2]$, which is the analogue of the component of the chain complex **1**. The geometries used were taken from the X-ray structural data of complex **1** and modified for $[Cu(NH_3)_4(H_2O)][Cu(ox)_2]$. The EHMO calculation (Figure 7c) showed that the HOMO (−11.81 eV) and LUMO (−11.04 eV) possess the $d_{x^2-y^2}$ orbital character of the $[Cu(ox)_2]^{2-}$ (Figure 7a) and $[Cu(NH_3)_4(H_2O)]^{2+}$ (Figure 7b) units, respectively, and this means that each magnetic orbital cannot mix, even if the HOMO and LUMO are separated by 0.77 eV. It is concluded that even a strong antiferromagnetic interaction cannot be attained in complex **1** with this bridging conformation.

The next step to prepare a ferromagnetic chain requires the construction of a one-dimensional compound with a short bond (e.g. Cu–O(3) in complex **1**) distance. It is known that a copper complex with bipyridine prefers to form a mono(bipyridyl) complex because the steric hindrance of an α-hydrogen of the bipyridine makes a bis(bipyridyl) complex unstable. In other words, the copper mono(bipyridyl) complex is very stable and has four more coordination sites. If the two oxalato groups coordinate to the copper atom as a bidentate ligand, each oxygen atom coordinates both from the d_{z^2} and $d_{x^2-y^2}$ direction. The remaining four terminal oxygen atoms might be used to bridge the next units; hence, a zigzag chain structure can be formed:

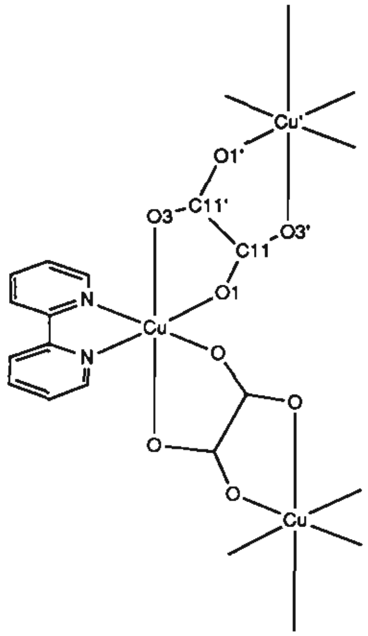

As the result of the bidentate nature of the oxalato groups, the bond length *d* (Cu–O(3) (d_{z^2} direction) becomes shorter and the values of bond angle θ_1 (Cu–O(3)–C(11′)) and dihedral angle θ_2 (the angle between the planes defined as Cu–O(3)–C(11′) and O(3)–C(11′)–C(11)) are expected to become suitable ones (110 and 0°, respectively) for σ-donation of O(3) atom. Complex **2** formulated as $[Cu(bpy)(ox)]\cdot 2H_2O$ has been proven to have a one-dimensional structure as stated in the previous section. The corresponding bond length (*d*), bond angle (θ_1), and dihedral angle (θ_2) for complex **2** are 2.314 (2) Å, 108.4 (1)°, and 2.7 (2) or 6.3 (2)°, respectively. In complex **2**, it should be noted that the bond length *d* becomes shorter and the bond and dihedral angles become closer to 110 and 0°, respectively. This bridging conformation makes the σ-donation of the terminal oxygen atoms

---

[47] Anderson, P. W. In *Solid State Physics*; Seitz, F., Turnbull, D., Eds.; Academic Press: New York, 1963; Vol. 14, p 99.

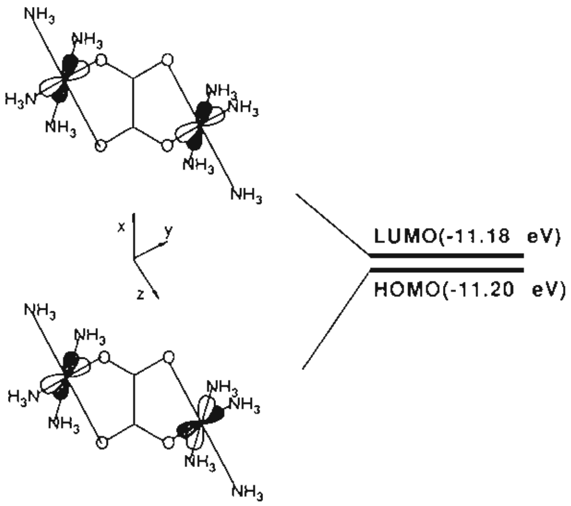

Figure 8. Extended Hückel MO diagram of $[Cu_2(NH_3)_8(ox)]^{2+}$.

stronger. The cryogenic magnetic measurement does show a ferromagnetic interaction, and the quantum number of the total angular momentum J at 2 K is confirmed to be higher than $^3/_2$.

Some mechanisms to explain the ferromagnetic interactions in acetato- or carboxylato-bridged copper(II) complexes ($[Cu(dien)OAc]_n(ClO_4)_n$[20] and Cu(pzdc)·HCl;[22] dien = diethylenetriamine, pzdc = 2,3-pyridinedicarboxylate) have been proposed. It has been suggested that the ferromagnetic interaction is propagated via a delocalized π-electron pathway of the bridging ligand. The dihedral angle between the plane of the acetate or carboxylate ligands and the plane containing the $d_{x^2-y^2}$ orbital is 90° in these complexes, and this results in the π system of the bridging ligand being orthogonal to the magnetic orbitals ($d_{x^2-y^2}$), hence, the propagation of the ferromagnetic interaction.[20,22] This explanation seems to be ambiguous for the following reason. The induction of spin in the p_π orbital by the spin on the $d_{x^2-y^2}$ orbital must be very small because these two orbitals are orthogonal. The propagation of a ferromagnetic interaction can be explained in our system as follows. All the oxygen atoms in the $[Cu(ox)]^{2+}$ unit have a substantial spin density on the p_σ orbitals (Table V). In complex **2** the spin density on the copper atom is delocalized to the neighboring copper atom through the σ-pathway of the bridging oxalato ligand. There are two types of σ-pathways (see above figure). The first is Cu–O(1)–C(11)–C(11′)–O(1′)–Cu′ or Cu–O(3)–C(11′)–C(11)–O(3′)–Cu′, and the second is Cu–O(1)–C(11)–O(3′)–Cu′ or Cu–O(3)–C(11′)–O(1′)–Cu′, where Cu′ belongs to the adjacent unit. In the first pathway, the O(1) and O(1′) (or O(3) and O(3′)) atoms coordinate to the copper atoms from the $d_{x^2-y^2}$ (or d_{z^2}) direction. This pathway results in an antiferromagnetic interaction because both copper atoms are in the $d_{x^2-y^2}$ ground state. The two bonds (Cu–O(1) and Cu′–O(1′) or Cu–O(3) and Cu′–O(3′)) are, however, separated by the C(11)–C(11′) bond, and this long pathway makes the antiferromagnetic interaction very weak. In the second pathway, the O(1) and O(1′) atoms coordinate to the copper atom from the $d_{x^2-y^2}$ direction, while the O(3) and O(3′) atoms coordinate to the copper atom from the d_{z^2} direction. The delocalized spin density on the O(3) or O(3′) atoms can induce spin on the d_{z^2} orbital of the adjacent copper atom, which is orthogonal to its $d_{x^2-y^2}$ orbital. The orthogonality between the d_{z^2} orbital of the induced spin and the $d_{x^2-y^2}$ orbital of the primary spin is responsible for the ferromagnetic interaction. The EHMO calculation of $[Cu_2(NH_3)_8(ox)]^{2+}$, which has geometry similar to the component of complex **2**, does show that the HOMO–LUMO energy gap is only 0.02 eV, and this value is considered to be small enough to favor the ferromagnetic interaction of complex **2**. It is not possible to predict the magnitude of the magnetic interaction by the EHMO calculation. The small J value for complex **2** can be explained by the fact that the ground state of the copper is not strictly $d_{x^2-y^2}$. A crystallographic study revealed that the bond angles around the copper atom deviate from 90° and the d_{z^2} axis is bent. This means that the mixing of d_{z^2} character into the $d_{x^2-y^2}$ orbital occurs. Therefore, the orthogonality of the two orbitals is not strictly kept and this causes a weak ferromagnetic interaction.

Conclusion

Extended Hückel molecular orbital calculation for the complex $[Cu(en)_2][Cu(ox)_2]$ (**1**) shows that the molecular orbitals of the cation and anion units do not mix. Hence, a very weak antiferromagnetic interaction was observed in complex **1**. In the complex $[Cu(bpy)(ox)]\cdot 2H_2O$ (**2**), the spin on the occupied d_{z^2} orbital is induced from the adjacent molecule and the orthogonality between the primary magnetic orbital ($d_{x^2-y^2}$) and the d_{z^2} orbital of the induced spin results in the ferromagnetic chain. It has been proven that modification of the bridging conformation makes the neighboring magnetic orbitals orthogonally aligned; hence, a ferromagnetic interaction can be propagated.[47]

Acknowledgment. We wish to express our thanks to Prof. Kazuo Kitaura (Institute for Molecular Science) for his help in the EHMO calculations. This work was supported in part by a Grant-in-Aid for Scientific Research on Priority Area (No. 228/04242225) from the Ministry of Education, Science and Culture of Japan, to which our thanks are due.

Supplementary Material Available: Tables SI–SXIV, listing X-ray data collection parameters, derived hydrogen positions, thermal parameters, bond distances and angles, and magnetic susceptibility data (10 pages). Ordering information is given on any current masthead page.